

Mechanical Characterization and Strain Analysis Applied to the Heat Treatment of Wood Materials, by Means of Digital Image Correlation

Deniz Aydemir,^{a,*} Oğuz Aksu,^a Timucin Bardak,^b Barbaros Yaman,^c Eser Sözen,^{a,g} Ömer Ümit Yalçın,^d Gökhan Gündüz,^e and Nurhan Koçan^f

Digital image correlation (DIC) was used to examine the strain distribution of heat-treated beech and Uludag fir woods in mechanical testing. It also evaluated the effects of the heat treatment process on the properties of the wood samples. The physical (mass/density loss, dimensional stability, color change, and surface roughness), mechanical (flexure test and compressive strength), morphological, thermal, and structural properties of the heat-treated wood were examined. It was determined that the heat treatment parameters can be optimized using the DIC method. The test results showed that although heat treatment can provide improved physical and thermal properties, it caused micro-crack formations and collapses in the wood cells. As a consequence, the mechanical properties of the heat-treated wood materials decreased with the heat treatment process. There were slight differences in the curves of the samples according to Fourier infrared and X-ray diffraction analyses. Morphological characterization showed that the heat treatment triggered large cracks in the cell wall and lumens and the morphological structure of heat-treated wood was affected at large percentages.

DOI: 10.15376/biores.19.2.3010-3030

Keywords: Bio-based construction materials; Decorative applications; Wood materials; Thermal modification; Material characterization

Contact information: a: Forest Industrial Engineering, Faculty of Forestry, Bartın University, 74100, Bartın, Turkey; b: Furniture and Design, Vocational School, Bartın University, 74100, Bartın, Turkey; c: Forest Engineering, Faculty of Forestry, Bartın University, 74100, Bartın, Turkey; d: Forest Industrial Engineering, Faculty of Forestry, Isparta University of Applied Sciences, 32100, Isparta, Turkey; e: Iskenderun Technical University, Faculty of Engineering and Natural Sciences, Department of Industrial Engineering, 31200 Iskenderun, Hatay, Türkiye; f: Department of Landscape Architecture, Faculty of Engineering, Architecture and Design, Bartın University, Bartın, Turkey; g: Forest Products Research & Application Center, Bartın University, 74100, Bartın, Turkey;

*Corresponding author: denizaydemir@bartin.edu.tr

INTRODUCTION

Wood materials have a cellular and layered structure and contain multi-compounds including lignin, cellulose, hemicelluloses, and various extractives. The wood cells are made of multi-compounds in various percentages according to wood types and the changes in their percentages determine various properties of wood materials such as physical, mechanical, chemical, structural, *etc.* Wood generally has been utilized in many industrial sectors including furniture, construction, decoration, *etc.*, due to its numerous advantages such as environmental-friendly, sustainability, easy processing, high strength, and modulus. (Hill 2007; Aydemir *et al.* 2010; Gündüz *et al.* 2011; Cheng *et al.* 2016).

However, wood has some disadvantages such as hygroscopic structure, low dimensional stability, weak resistance to fungal degradation or insect damage, and flammability. Therefore, various preservation methods, including impregnation using protective chemicals, coating with dyes or varnish, heat treatment at high temperatures, or chemical modification, have been applied to the wood material in various application areas. Heat or thermal treatment has been studied for a long time because of its environment-friendly process, providing good dimensional stability, and ease of application (Hill 2007; Esteves and Pereira 2009).

Heat treatment limits the wood-water relationship of wood cells and provides lower-dimensional change due to permanent degradation in wood chemical structure. The treatment at high temperatures of wood generally results in dehydration, depolymerization, and finally thermal degradation of wood components including cellulose, hemicellulose, and lignin (Esteves and Pereira 2009; Kučerová *et al.* 2016). When wood is heated from room temperature to 160 °C, water, and various volatile compounds in wood are removed. While the temperatures are increased from 160 to 200 °C, hemicelluloses degrade, and the formation of acetic acid starts due to thermal degradation. The hemicellulose degradation generally causes a decrease in the bending properties of wood (Bekhta and Niemz 2003; Boonstra *et al.* 2007; Esteves *et al.* 2013). At temperatures above 220 °C, chain scission of cellulose starts to occur, and the degradation of cellulose leads to a decrease in the degree of polymerization (DP). The degradation results in a decrease in the tensile properties of wood (Tumen *et al.* 2010; Aydemir *et al.* 2011; Kačíková *et al.* 2013; Pelaez-Samaniego *et al.* 2013; Kučerová and Výbohová 2014). Percentages of lignin in wood increase with both hemicellulose and cellulose degradation (Hill 2007; Tumen *et al.* 2010). At 250 °C and above, lignin degradation starts to occur (Brebú and Vasile 2010), and the dominant reactions in the degradation occur generally in cross-linking ways (Nuopponen *et al.* 2005; Hill 2007; Tumen *et al.* 2010). Based on a review of the literature, the various studies on the physical (Nuopponen *et al.* 2005; Kučerová *et al.* 2016; Li *et al.* 2017), mechanical (Kubojima *et al.* 2000; Mburu *et al.* 2008; Kučerová *et al.* 2016; Percin *et al.* 2016), chemical (Boonstra and Tjeerdsma 2006; Mitsui *et al.* 2008; Inari *et al.* 2009; Brosse *et al.* 2010; Chien *et al.* 2018), thermal (Bhuiyan *et al.* 2001; Priadi and Hiziroglu 2013; Martinka *et al.* 2014; Czajkowski *et al.* 2020), structural (Bhuiyan *et al.* 2001; Cheng *et al.* 2016), and morphological (Awoyemi and Jones 2011; Priadi and Hiziroglu 2013) characteristics were conducted and the results showed that the heat treatment provided improved dimensional stability and enhanced durability to wood materials. There have been many studies on the material characterization of heat-treated wood. However, there is a lack of information related to the strain distribution during the heat treatment process of wood with digital image correlation (DIC) in the mechanical properties of heat-treated wood with the DIC technique. In this study, the effects of heat treatment on the physical, mechanical, thermal, structural, and morphological properties of wood materials were investigated, and DIC analysis was conducted in the mechanical testing and heat treatment process of wood materials.

EXPERIMENTAL

Materials

Kiln-dried beech (*Fagus orientalis* L.) (B) and Uludag fir (*Abies nordmanniana* subsp. *bornmulleriana* Mattf.) (UF) woods were supplied as lumber at dimensions of 150

x 60 x 500 mm from a local timber mill, Bartın, Turkey. Both wood types were cut to non-defect samples at dimensions of 25 x 25 x 400 mm and conditioned in a climatic chamber at 20 °C and 65% relative humidity.

Thermal Modification

Heat treatment (HT) was applied to the wood materials at dimensions of 25 x 25 x 400 mm in the presence of water vapor and air under room conditions in a controlled oven. The HT process was conducted at 170, 190, and 210 °C for 4 h to understand the effects of material properties of the Uludag fir and beech woods. After HT, the samples were conditioned until they reached 12% moisture content (MC), and they were resized by planing and sanding to match the same dimensions for testing to obtain the standard test samples presented in the method section. Test samples were coded as Uludag fir wood treated at 170°C (UF-170), 190°C (UF-190) and 210° (UF-210) and beech wood treated at 170 °C (B-170), 190 °C (B-190), and 210 °C (B-210), un-treated Uludag fir (UF-C), and un-treated Beech (B-C).

Methods

Physical properties

The density of the un-treated and heat-treated woods was determined according to ISO 4859 (1982) and ISO 13061-2 (2014) methods. The water absorption, swelling, and shrinkage tests were conducted in 15 samples replicated using ISO 4859 (1982). The color changes were detected on the sample surfaces before and after the treatment by a Minolta Chroma-Meter CR-300 colorimeter (Chiyoda, Tokyo) using a D65 illuminant and a 10-standard observer. The changes in the L^* , a^* , and b^* axes were shown as ΔL^* , Δa^* , and Δb^* according to DIN 5033-1 (2017). The surface roughness was determined by a touch scan device (TIME TR200) according to the ISO 4287 (1997). The roughness parameters include the average of profile height deviations from the mean line (R_a), root mean square average of profile height deviations from the mean line (R_q), and maximum peak to valley height of the profile, within a sampling length (R_z) were measured.

Mechanical properties

Compression and bending test samples were prepared as $2 \times 2 \times 3$ cm and $2 \times 2 \times 36$ cm³ dimensions and conditioned until reaching 12% MC in a climatic cabinet. Flexural and compressive tests were conducted on an Utest mechanical tester 10 kN testing machine according to ISO 3349 (1975), ISO 3133 (1975), ISO 3345 (1975), respectively. For both flexural and compressive tests, the speed of the mechanical tester was set as 5 mm/min. Twenty replicates were used for all mechanical properties.

Thermogravimetric analysis (TGA)

The TGA of the un-treated and heat-treated wood materials was evaluated within a temperature range of 10 °C from room temperature to 600 °C *via* a thermogravimetric analyzer. Measurements were performed on samples with 1.0 to 2 mg weight in a Perkin Elmer test device (Waltham, MA, USA). The degradation temperature at 10%, 50%, and 80% weight loss (WL) ($T_{10\%}$, $T_{50\%}$, and $T_{80\%}$) at the decomposition stages and the maximum degradation temperature (DTG_{max}) were detected.

X-ray diffraction (XRD)

The XRD patterns were obtained with an X-ray diffractometer (Model XPert PRO, Philips PANalytical, Netherlands) from 5° to 90° 2 θ range. In all analyses, the same sample holder and their position were used. The crystallinity index (CI) and crystal size (CS) were calculated using the formulation given in Eq. 1,

$$CI_{(\%) } = \frac{\Sigma A_c}{\Sigma(A_c+A_a)}, \quad CS_{nm} = \frac{K \cdot \lambda}{\beta \cdot \cos(\theta)} \quad (1)$$

where CI (%) was calculated with the integrated area of the respective crystalline peaks (A_c) and the amorphous halo (A_a). The Bragg angle for the reflection (θ), the wavelength of radiation (0.15406 nm) (λ), the integral breadth at the half-maximum intensity in radians (β), and the Scherrer parameter (K) were used to calculate the CS (nm).

Fourier transform infrared spectroscopy (FTIR)

The FTIR was conducted with a Shimadzu IRAffinity-1 spectrometer equipped with a single reflection AT-IR pike MIRacle sampling accessory. The sampling was obtained at wavenumbers from 800 to 4000 cm⁻¹. The arithmetic means of four replicates for the samples were used in the study.

Scanning electron microscopy (SEM)

The SEM images were obtained with a Tescan spectroscopy (Brno, Czech Republic). The mixture of Palladium/Gold particles was coated on the sample to increase the flowing of the electron (Tescan group, MAIA3 XMU).

Digital image correlation (DIC)

A digital camera, which has a color view, 1624 × 1234 megapixels, 20 fps, was used to capture the images of the un-treated and heat-treated wood materials after the bending test was finished. White-black dots on the surface of the samples were created with a metallic foam to detect the strain that occurred during the thermal treatment and mechanical test. Ncorr software (LabVIEW, National Instruments, Austin, TX, USA) was used to detect the changes in the location of the dots during the DIC analysis. The strain along the X-direction (\mathcal{E}_{xx}), shear strain (\mathcal{E}_{xy}), and strain along the Y-direction (\mathcal{E}_{yy}), was calculated according to previous studies (Pan *et al.* 2009; Canal *et al.* 2012; Caminero *et al.* 2013; Harilal *et al.* 2015; Yoneyama *et al.* 2016; Guoqing Gu *et al.* 2017; Barile *et al.* 2019).

RESULTS AND DISCUSSION

Figures 1 (a), (b), and (c) show the drying strains of wood materials with the DIC method in the heat treatment. The DIC method successfully detected the strain distribution directions including \mathcal{E}_{xx} , \mathcal{E}_{xy} , and \mathcal{E}_{yy} . The maximum and minimum strain values were colored in red and blue, respectively. In the direction of \mathcal{E}_{xx} , several strain distributions were detected to be low at 170 °C due to vaporizing extractive compounds in wood and a decrease in the moisture content of wood materials. At 190 °C, the strain distribution rose, and the strain distribution increased to its highest level at 210 °C. The beech wood was affected higher than Uludag fir due to the heat treatment process. In both wood types, the strain distribution was more homogenous at 210 °C. As can be seen in the direction of \mathcal{E}_{xy} ,

the strain distribution was heterogeneously placed in various sections of the wood materials. According to the direction of the ϵ_{yy} , the strain distribution was detected in various parts of both wood materials and the high strain distribution was generally in Uludag fir wood at 190 and 200 °C. The strain distribution in ϵ_{yy} of beech wood was lower than in Uludag fir wood.

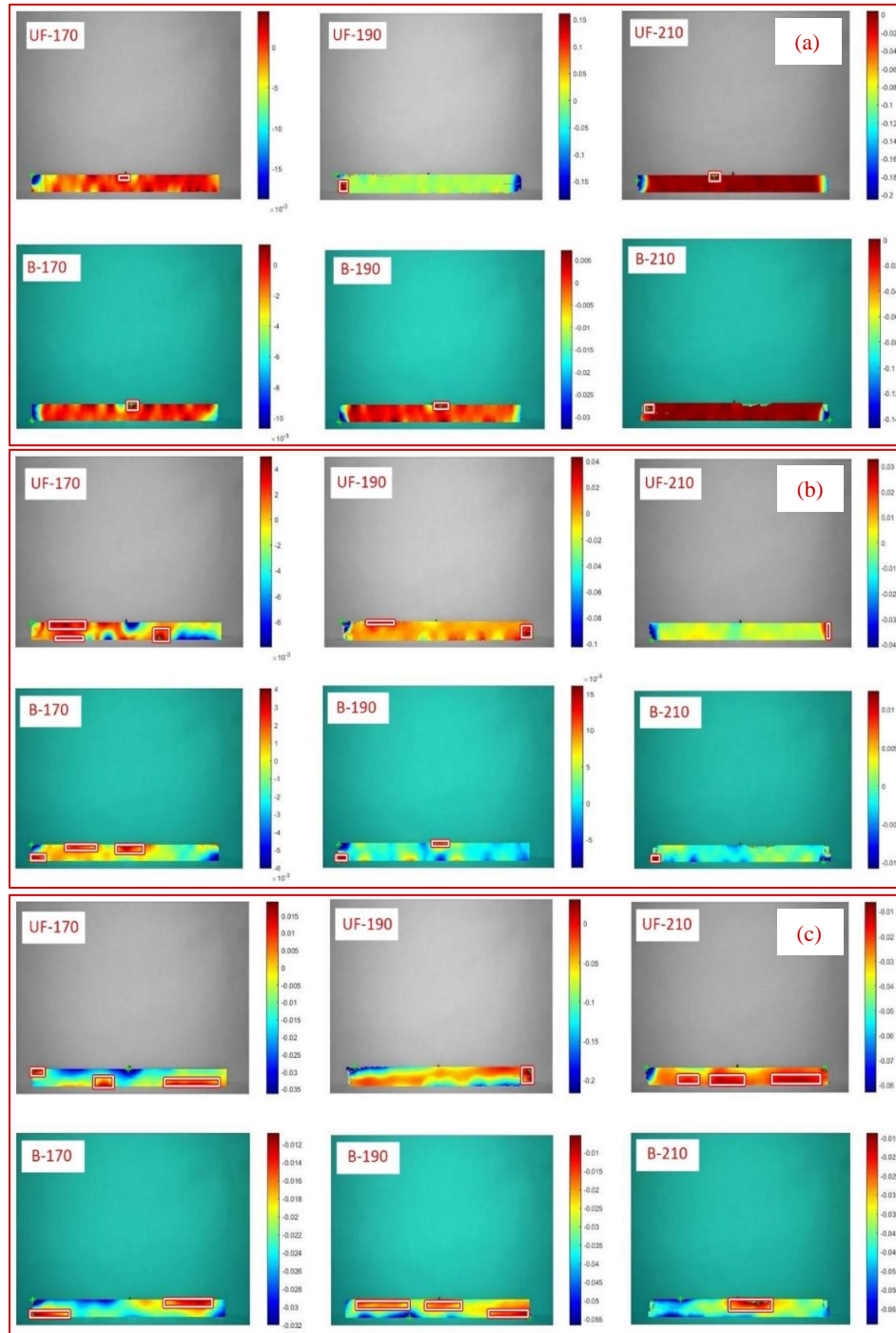


Fig. 1. Strain distributions in ϵ_{xx} (a), ϵ_{xy} (b) and ϵ_{yy} (c) in the heat treatment (UF: Uludag fir, B: beech)

The study revealed that strain distributions in the direction of ϵ_{xx} , ϵ_{xy} , and ϵ_{yy} varied at different temperatures in both types of wood. This finding is consistent with previous research that used the DIC method to comprehensively characterize the elastic behavior of European beech (*Fagus sylvatica* L.) under three different heating intensities. The researchers found that the heat treatment affected the elastic behavior of the material. However, the effect of the treatment varied among the elastic components, with non-uniform trends with the intensity of the heat treatments (Gómez-Royuela *et al.* 2021). Figure 2 shows some physical properties including mass and density loss, dimensional stability, color change, and surface roughness of heat-treated wood materials.

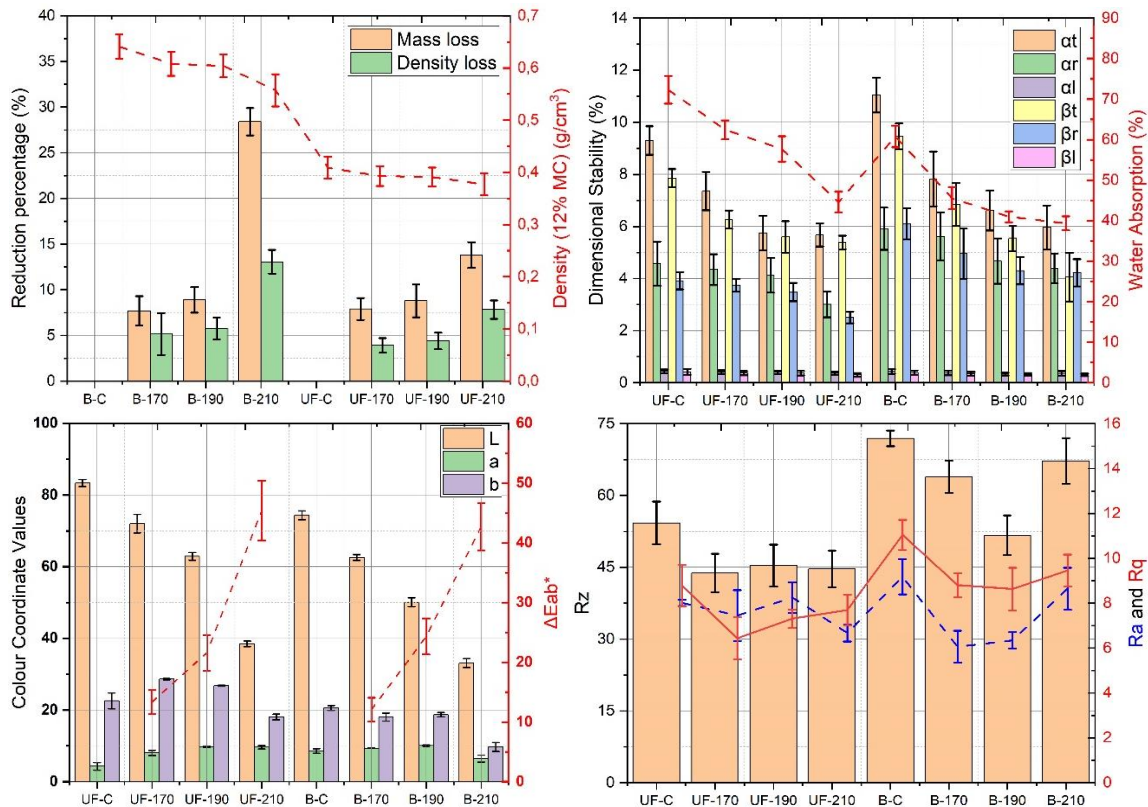


Fig. 2. Some physical properties of heat-treated woods (UF: Uludag fir, B: beech)

According to Fig. 2, the density decreased for both kinds of wood with heat treatment. Mass losses in both wood types also caused density losses. The mass loss increased more by the degradation of main components in wood from 170 to 210 °C of temperature (Gündüz and Aydemir 2009; Kaygin *et al.* 2009; Nhicila *et al.* 2020). The highest mass and density loss was determined as 28.4% and 13.1% in beech wood at 210 °C, respectively. The water absorption of both kinds of wood decreased with the treatment and the lowest water absorption value was found at 39.3% for beech wood treated at 210 °C. Previous studies showed that heat-treated wood has decreased hydrophobicity and density due to the removal of volatile compounds and thermal deterioration of the main components, and the free hydroxyl groups in celluloses had a statistically a significant effect on the wood-water relationship. Heat treatment decreases water absorption and improves dimensional stability because of the decrease in the number of hydroxyl groups (Gündüz and Aydemir 2009a; Gündüz *et al.* 2009; Nhicila *et al.* 2020). After the treatment,

it was observed that the color changes increased due to thermal degradation of the main chemical components of wood, and considering the total color changes, the color changes of both wood types increased with heat treatment, and the color change rate of Uludag fir wood treated at 210 °C was higher than beech wood treated at 210 °C. Although this may seem like a negative situation because it makes the wood material darker, it will visually make it an alternative material in exterior coatings or decorative applications, or interior/exterior designs. The surface roughness of both wood after the treatment was investigated and the surface roughness parameters including R_z , R_a , and R_q of the heat-treated samples were lower than the un-treated samples. The decrease in the surface roughness is caused by the heat treatment resulting in a plasticization of the wood surfaces. Lignin softens at temperatures above 160 °C and thus densifies the heat-treated wood surface, and the surface of heat-treated wood becomes rough (Korkut *et al.* 2008). Figure 3 shows the mechanical properties of the samples.

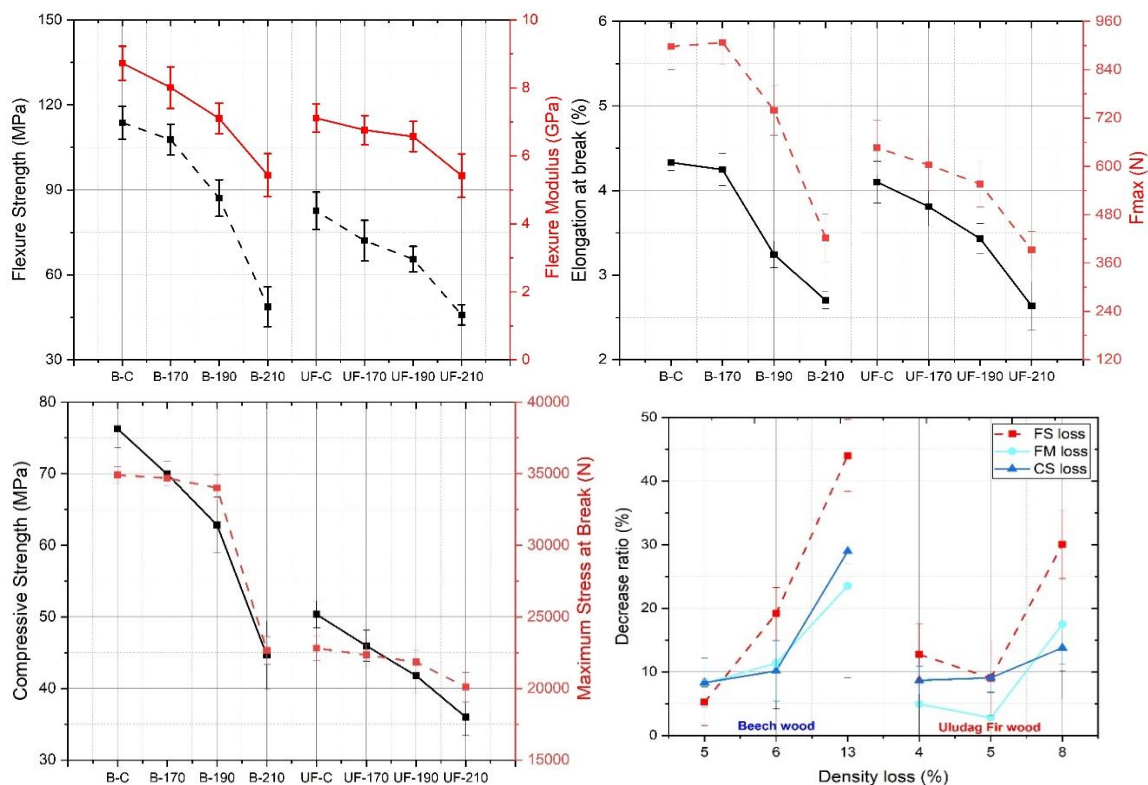


Fig. 3. Mechanical properties of the heat-treated and un-treated wood samples (FS loss: flexure strength loss, FM: flexural modulus loss, CS loss: compressive strength loss)

The changes in the mass and density that occurred with the heat treatment affect the mechanical properties of wood materials, and therefore, the mechanical properties including bending strength, bending modulus, and compression strength of the samples are given in Fig. 3. Bending strength and modulus were decreased when the treatment temperature was raised from 170 to 210 °C, and the lowest bending strength and modulus were found at 48.8 MPa (– 57.1%) and 5.4 GPa (– 37.9%) for beech wood treated at 210 °C and 45.9 MPa (– 44.5%) and 5.4 GPa (– 23.9%) for Uludag fir wood treated at 210 °C, respectively. The obtained results showed that the decreasing trend in the bending strength and modulus after the heat treatment was similar to each other, but the decrease rate in the

Beech wood was higher than in Uludag fir wood due to its high mass or density loss. In the bending test, both elongation at break and F_{\max} exhibited a similar trend to the changes in bending strength and modulus. As can be seen in compression strength results, heat treatment caused a decrease in the compression strength, and the compression strength decreased more while treatment temperatures were raised from 170 to 210 °C. The lowest compression strength was found at 44.6 MPa (– 41.5%) for beech wood and 36 MPa (– 28.4%) for Uludag fir wood. The wood types treated at 170, 190, and 210 °C became tiny cracks and collapsed on the cell wall. These defects could negatively affect the mechanical properties of the heat-treated woods (Xing *et al.* 2016; Chen *et al.* 2020) and also the mechanical properties of beech wood were lower than in Uludag fir wood due to high-density loss and thermal degradation caused by complex structure and wood constitutes of hardwoods (De Oliveira Araújo *et al.* 2016; Gennari *et al.* 2021). The deformation and strain distribution that occurred in the bending test of heat-treated and un-treated woods were investigated with the DIC method as given in Fig. 4.

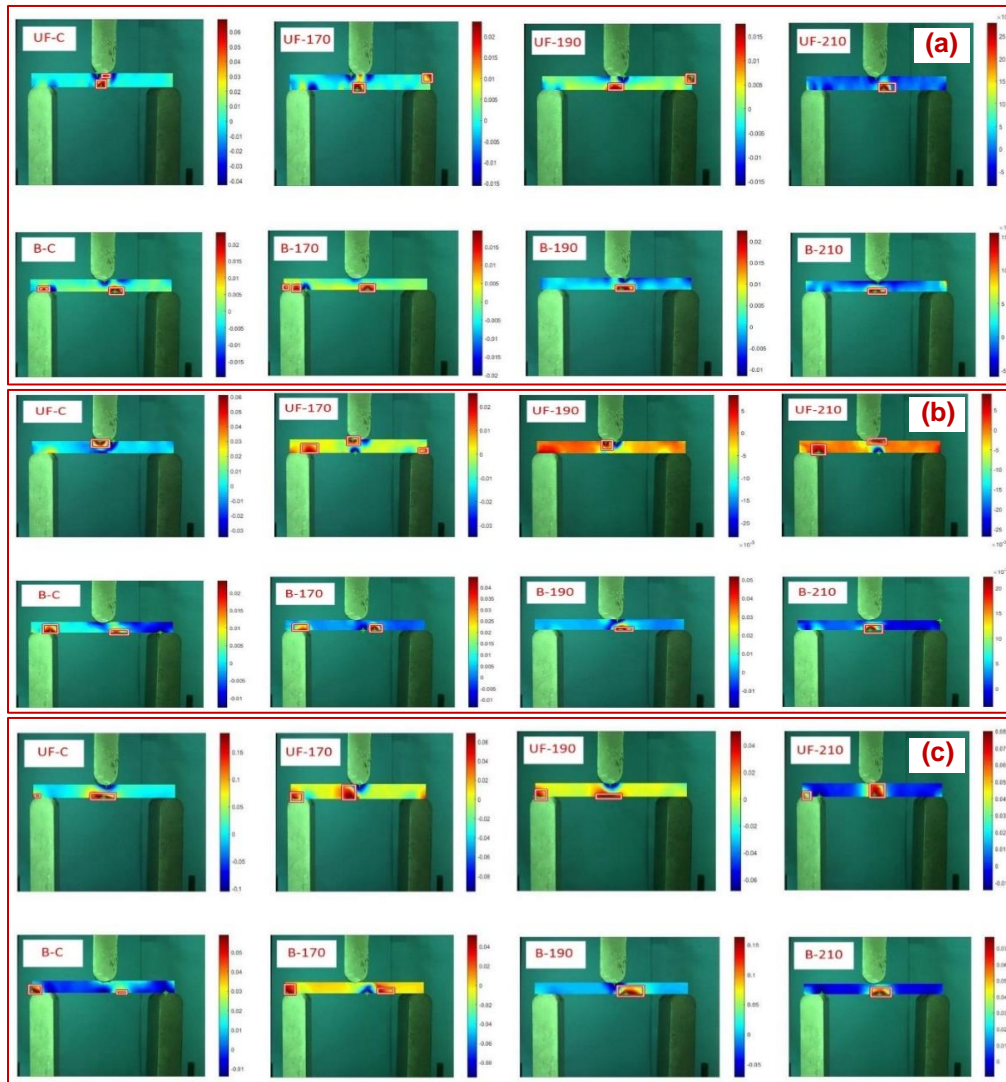


Fig. 4. Strain distributions in ϵ_{xx} (a), ϵ_{xy} (shear) (b), and ϵ_{yy} (in the Y-direction) (c) under the maximum loading (F_{\max}) in the bending test (the scale information changes from -0.005 to 0.06 and the scale shows the strain in the bending test)

When the strain distributions of ϵ_{xx} were examined under F_{max} during the bending test (Fig. 4a), the strain was more homogeneously distributed at the highest temperature values in both pine and beech wood materials, and the strain generally was concentrated in a few areas. The strains generally were located near load cell or the supports. The ϵ_{xy} strain distributions were examined under F_{max} in the bending test (Fig. 4b). The strain generally was concentrated in some location of the beech wood material. However, the strain distribution was heterogeneously dispersed on the Uludag fir wood. The ϵ_{xy} strain distributions were seen to concentrate at near load cells or the supports in a similar way to ϵ_{xx} . When the ϵ_{yy} strain distributions were examined under F_{max} in the bending test (Fig. 4c), the strain was more homogeneously distributed at the highest temperature values in both pine and beech wood materials. The strain distribution in Uludag Fir wood was generally higher than in beech wood. The DIC method was successfully used in both the heat treatment process and strain determination in the bending test. The heat treatment to be used to reduce the disadvantages of wood materials in outdoor applications can be optimized by using the DIC methods, and it can be said that important information can be obtained from the DIC method to design structural wood materials (Jeong and Park 2016). The curves for TGA and DTG of the samples are presented in Fig. 5. The summary of thermal stability for the samples is given in Table 1.

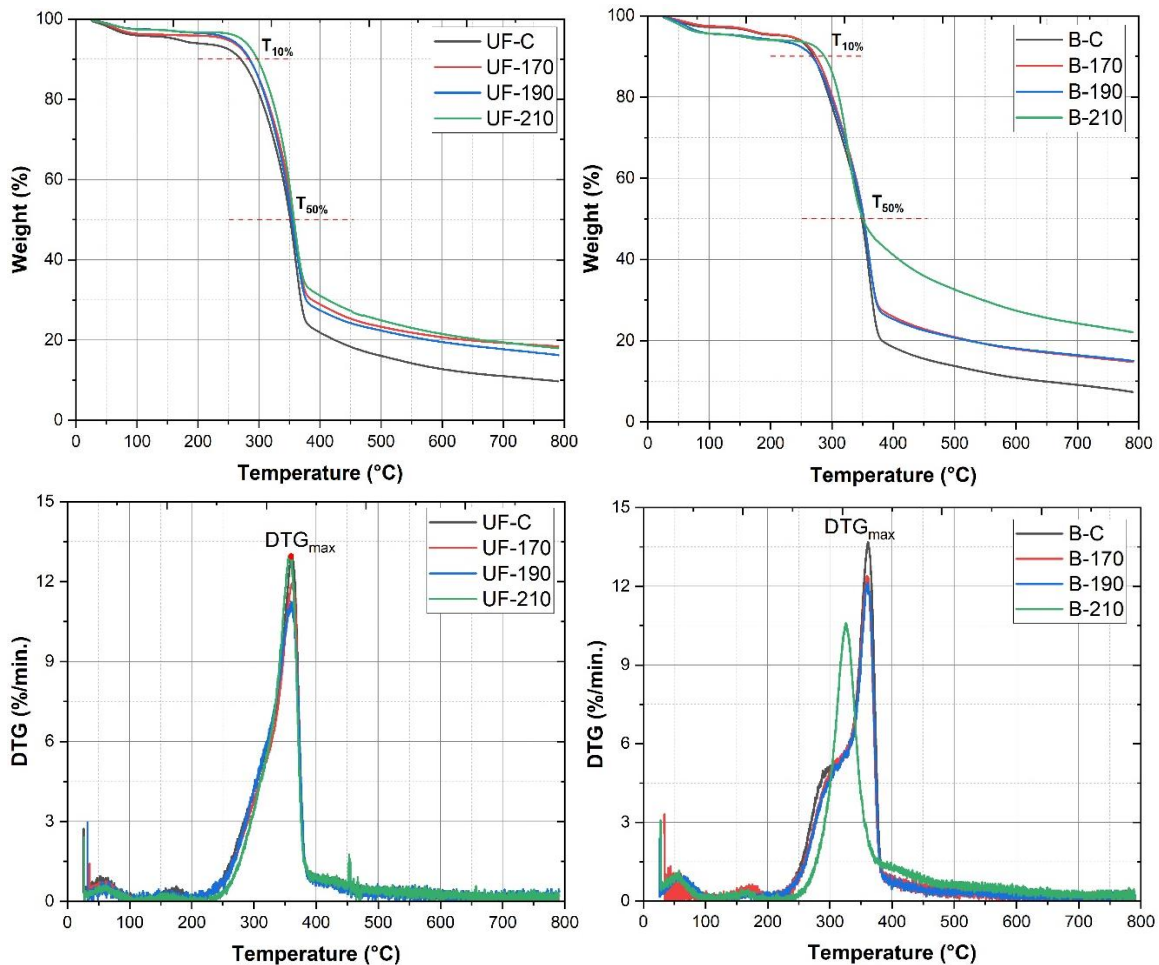


Fig. 5. The curves for TGA and DTG of the samples

As can be seen in Fig. 5, TGA curves of the woods were nearly similar to each other, but weight loss (WL) amounts were generally changed according to the treatment temperature and wood types. The degradation behavior of the woods exhibited three regions in TGA and DTG curves that showed the thermal degradation of the organic constituents and volatile compounds in the wood structure (Marková *et al.* 2018). TGA and DTG curves showed the evaporation of water and extractive materials of woods in the 1st region between 50 and 200 °C. The degradation of wood accounts for the second region between 250 and 400 °C, and the decomposition of wood constitutes in the third region above 400 °C, as given in Fig. 10. The TGA of the wood exhibits three stages for mass loss behavior (Yang *et al.* 2005; Karakus *et al.* 2016). The evaporation of water and volatile compounds starts at 100 °C, and then the thermal degradation of the essential constituents occurs between 150 and 350 °C for hemicelluloses, between 240 and 350 °C for cellulose, and between 250 and 500 °C for lignin (Kaboarani and Faezipour 2009; Aydemir *et al.* 2011). The degradation behavior obtained in this study was generally in agreement with the results reported in the literature (Aydemir *et al.* 2011, 2015; Marková *et al.* 2018).

Table 1. Thermal Properties for the Untreated and Heat-Treated Wood Materials

Samples	$T_{%10}$ (°C)	$T_{%50}$ (°C)	$T_{%80}$ (°C)	DTG _{max} (°C)	Residual mass (%)
UF-C	270.4	351.5	529.7	361.5	9.7
UF – 170	284.2	357.1	643.3	361.7	18.4
UF – 190	284.8	353.9	579.4	359.3	16,2
UF – 210	297.2	357.3	665.4	358.1	18
B – C	269.7	348.5	381.5	361.2	7.4
B – 170	273.2	351.3	525.1	358.7	14.8
B – 190	267.6	351.7	523.2	360.7	15
B – 210	287.7	350.4	> 800	325.5	22.1

As can be seen in Table 1, all degradation temperatures including T10%, T50%, and T80% generally increased with the treatment temperatures, and the highest temperatures for T10%, T50%, and T80% were determined at 297.2 °C for UF-210, 357.3 °C for UF-210, and > 800 °C for B-210, respectively. DTG_{max} of heat-treated samples was lower than the un-treated samples and finally, the weight loss decreased with the treatment and the decreasing rate increased with treatment temperatures. The highest and lowest weight loss was calculated as 92.6% for B-C and 77.9% for B-210, respectively. As seen in the obtained result, it can be said that the thermal treatment increased the thermal stability of wood materials. Figures 6 (a) and (b) show the XRD graphs of heat-treated and untreated Uludag fir and beech woods, respectively. Uludag fir and beech exhibited two peaks at around 15° and 22° in the XRD graph. No difference was noticed between different heat treatments for the same wood species, and the pattern was generally similar to each other. However, there were some differences for intensities in the curves of the samples. In XRD, the crystallinity index and crystal size of the materials can be calculated. The crystallinity index is known as the ratio of crystalline peak to crystalline and amorphous peaks.

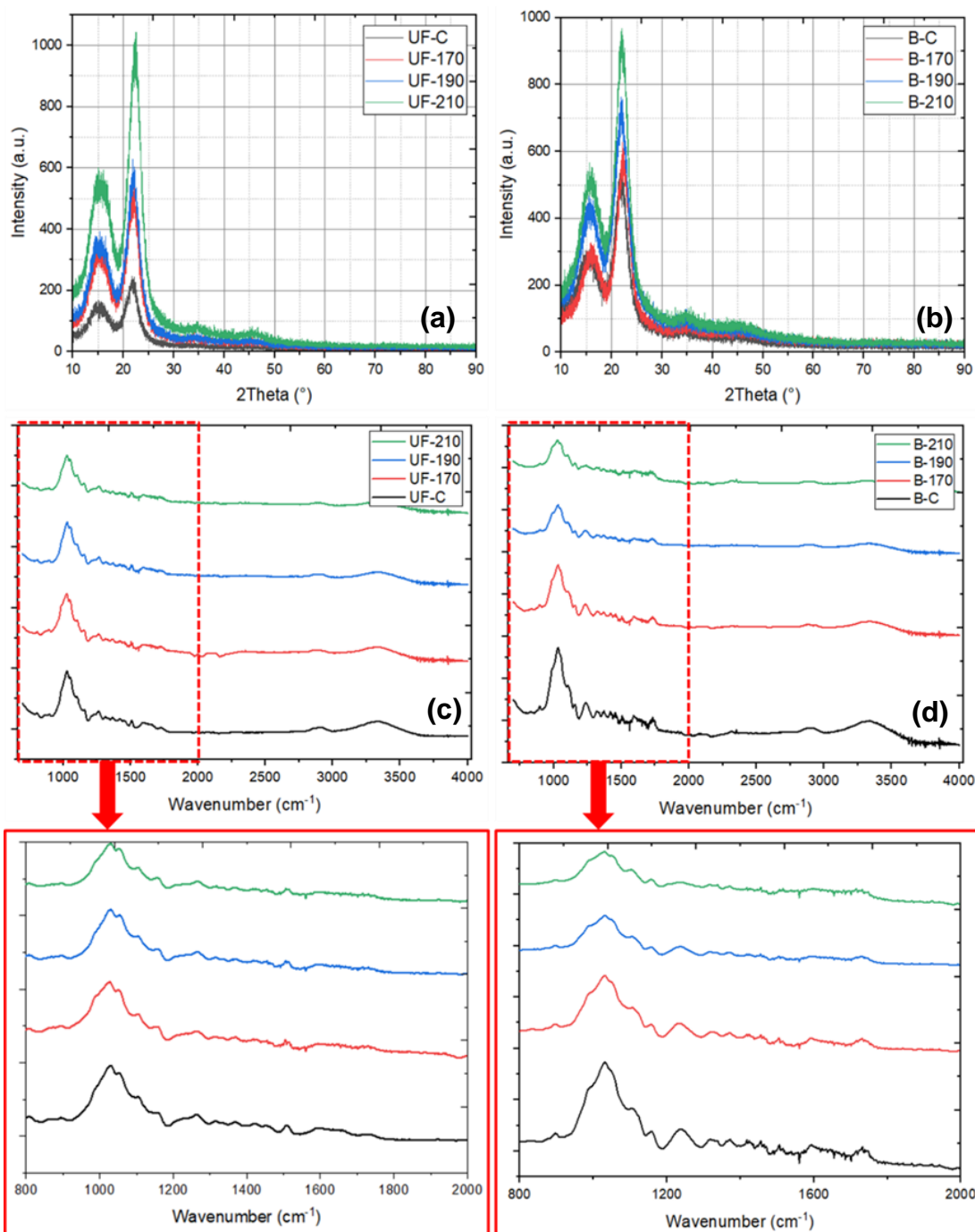


Fig. 6. XRD patterns (a) for Uludag fir and (b) for beech; and FTIR spectra (c) for Uludag fir and (d) for beech

The crystallinity index of wood materials changes with the treatment conditions according to previous studies (Aydemir *et al.* 2015; Karakus *et al.* 2015). Therefore, the crystallinity and crystal sizes were measured with XRD after heat treatment of wood materials. As can be seen in Table 2, 2θ ranged from 15.2° to 15.9° to 21.9° to 22.3° . The crystallinity increased with thermal treatment, and while the thermal treatment increased, the crystallinity generally continued to increase. The highest crystallinity was calculated as

64.2% for Uludag fir and 57.9% for beech. The crystal size ranged from 2.90 nm to 2.95 nm for UF, and 2.76 nm to 2.89 nm for B, respectively.

Table 2. Crystallinity and Crystal Sizes Measured with XRD after Heat Treatment of Wood Materials

Samples	2 θ^* ($^{\circ}$)	Crystallinity (%)	Crystal Size (nm)
UF-C	15.2, 21.9	64.1	2.90
UF – 170	15.5, 22.1	63.8	2.90
UF – 190	15.3, 22.1	64.2	2.95
UF – 210	15.6, 22.3	64.9	2.92
B – C	15.6, 22.0	55.8	2.81
B – 170	15.9, 22.2	57.1	2.84
B – 190	15.5, 21.9	56.7	2.76
B – 210	15.6, 22.0	57.9	2.89

*In XRD graph, two crystalline planes at 2 θ degrees were detected.

Figures 6 (c) and (d) show the FTIR spectra of heat-treated and untreated Uludag fir and beech samples, respectively. The spectra of the untreated and heat-treated wood exhibited a similar structure. They did not indicate any different peaks in the graphs, but some slight peak shifts in the intensity of some peaks were observed after the treatment. The characteristic bands and their assignment that were detected for the un-treated wood with FTIR are given in Table 3. In the spectra, firstly, the bands for Uludag fir and beech at 3340 and 3342 cm^{-1} were assigned to the O–H stretching, and the bands at 2903 and 2902 cm^{-1} were assigned to the C–H stretchings in CH_2 and CH_3 , respectively (Esteves *et al.* 2013; Chien *et al.* 2018; Aytakin and Yazıcı 2021). The bands at 1734 and 1732 cm^{-1} were assigned to C=O stretching of carboxyl groups and acetyl groups in hemicellulose. Acetyl ($\text{CH}_3\text{C}=\text{O}$) absorption was higher for beech wood than that of Uludag fir wood and the band intensity of wood types decreased with increasing temperatures. This may be caused due to deacetylation of hemicellulose by cleavage of acetyl groups that occurred in the course of heat treatment (Bekhta and Niemz 2003; Altgen *et al.* 2018). When treatment temperatures reached 210 $^{\circ}\text{C}$, the samples slightly shifted to lower wavenumbers. Aromatic skeletal stretching bands for lignin were assigned at 1595 and 1592 cm^{-1} for Uludag fir and beech woods, respectively. The band intensity rose with an increase in the temperature due to the relative ratio of lignin increased with the degradation of cellulose and hemicellulose. The other aromatic ring-stretching band was assigned at 1509 cm^{-1} and 1506 cm^{-1} due to guaiacyl-type and guaiacyl/syringyl-type lignin for Uludag fir and beech wood (Tjeerdsma and Militz 2005). The band intensity increased from 170 to 210 $^{\circ}\text{C}$ for both wood types and the band intensity at 260 $^{\circ}\text{C}$ decreased due to the syringyl unit of lignin thermally decomposing more rapidly than the guaiacyl unit, as explained by Faix *et al.* (1990), Esteves *et al.* (2013), and Chien *et al.* (2018). The bands at 1452 cm^{-1} (Uludag fir) and 1457 cm^{-1} (beech) were related to C–H deformation in lignin and xylan, and the bands at 1424 and 1423 cm^{-1} were assigned to aromatic skeletal stretching and C–H in-plane bending in lignin and carbohydrates, respectively (Faix *et al.* 1990; Tjeerdsma and Militz 2005; Windeisen *et al.* 2007; Altgen *et al.* 2018; Chien *et al.* 2018). The other characteristic bands are C-H bending, $-\text{CH}_3$ (lignin), $-\text{CH}_2$ (carbohydrates), lignin-carbohydrate complexes bonds for 1370 cm^{-1} (Tjeerdsma *et al.* 1998; Esteves *et al.* 2013), C-O deformation in cellulose, symmetric C-O-C, stretching of dialkyl ethers, aromatic C-H deformation in lignin in wavenumbers of 1026 to 1030 cm^{-1} (Esteves *et al.* 2013; Chien *et*

al. 2018), and alkyl-aryl-ether bonds, as well as lactones in wavenumbers of 1225 to 1235 cm^{-1} (Hakkou *et al.* 2005; Gonultas and Candan 2018). Table 3 shows the important bands and their assignments according to the literature review.

Table 3. Assignments for FT-IR Spectral Bands of the Wood Materials

Wavenumber (cm^{-1})		Assignments	References
Uludag Fir	Beech		
897	896	C–H bending and asymmetric out-of-plane ring stretching of cellulose	(Tjeerdsma <i>et al.</i> 1998; Windeisen <i>et al.</i> 2007; Esteves and Pereira 2009; Esteves <i>et al.</i> 2013; Aydemir <i>et al.</i> 2015; Gonultas and Candan 2018; Aytekin and Yazıcı 2021)
1030	1034	C–O deformation in $-\text{CH}_2\text{OH}$, C=O stretching, and aromatic C–H in-plane deformation	
1157	1157	C=O stretching in aliphatic and C–O–C stretching in pyranoses	
1233	1235	C–C, C–O, and C=O stretching of xylan and lignin	
1267	-	Guaiacyl ring breathing, C=O stretching in lignin, and C–O linkage in guaiacyl aromatic methoxyl groups	
1316	1317	$-\text{CH}_2$ wagging in cellulose and hemicellulose	
1370	1371	Aliphatic C–H stretching in methyl and phenolic OH	
1424	1423	Aromatic C–H stretching and C–H in-plane bending in lignin and celluloses	(Faix <i>et al.</i> 1990; Tjeerdsma and Militz 2005; Esteves <i>et al.</i> 2013; Altgen <i>et al.</i> 2018; Aytekin and Yazıcı 2021)
1452	1457	C–H deformation in lignin and xylan	
1509	1506	Aromatic C–H stretching of lignin	
1595	1592	Aromatic C–H stretching of lignin	
1734	1732	C=O stretching of carboxyl (R–COOH) groups and acetyl ($-\text{COCH}_3$) groups of hemicelluloses	(Bekhta and Niemz 2003; Chien <i>et al.</i> 2018)
2903	2902	C–H stretching in CH_2 and CH_3	(Esteves and Pereira 2009; Esteves <i>et al.</i> 2013; Aytekin and Yazıcı 2021)
3340	3342	O–H stretching	

Heat treatment affects the morphological structure of wood materials because of the thermal degradation of wood cells' constituents. The changes in the morphological structure were investigated with SEM as given in Figs. 7 (a), (b), (c), and (d). As can be seen in Fig. 7 (a), the early and latewood of control woods appeared to be smooth, and there are no micro-cracks in wood cells. In addition, the distances between the wood cells are normal and have similar thicknesses. After the heat treatment process, micro-cracks, cell ruptures, and cell collapses in the wood cells were detected. While the treatment temperatures were raised from 170 to 210 $^{\circ}\text{C}$, the degradation and the deterioration increased. Micro-cracks and cell ruptures were observed in the middle lamella of the cells.

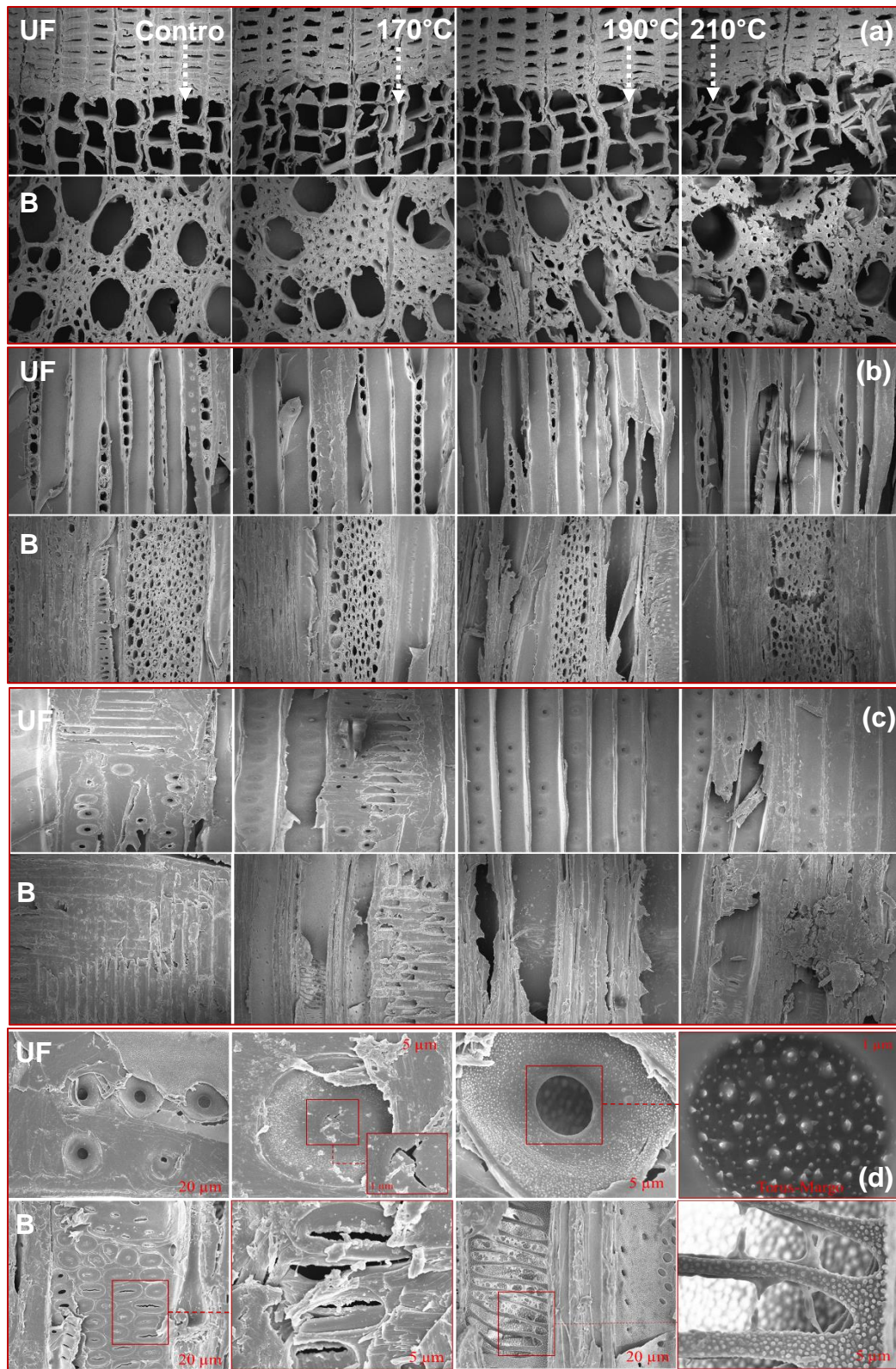


Fig. 7. Morphological changes in the cross-section (50 μm) (a), the tangential section (50 μm) (b), the radial section (50 μm) (c), and the changes in the pits between the cells (20, 5 and 1 μm) (d) of Uludag fir and Beech woods

It was also seen that some cells were individualized and filled into the lumens. Although similar structural deteriorations were apparent in both species, it was seen that these deteriorations were more apparent in the early wood of the Uludag fir wood due to high thermal deterioration. As seen in Fig. 7(b), it is observed that there were various deteriorations and micro-cracks in the parenchyma cells of Uludag fir wood as a result of heat treatment. Especially with the increase in the treatment temperature, this damage and deterioration increased even more. Although the same situation was detected in beech wood, the structural deterioration of beech wood in the tangential direction was much more than that of fir wood. When looking at SEM images in the radial direction of both kinds of wood as seen in Fig. 7(c), the deterioration was detected to be less for both wood types in this direction. Various micro-cracks and disintegration were detected in this section of both wood types. The pits between the cells of both wood types were examined according to the SEM pictures given in Fig. 7(d). It was seen that there were some micro-cracks in the pit edges of the Uludag fir wood and in the torus, and various amounts of cracks on the torus (the pit membrane that separates the bordered-pit pair) and margo (porous membrane in wood pits) after the treatment. In addition, ruptures and cell disintegration in the cell-pit conjunctions were detected. When looking at the beech wood, it was determined that the pits were usually blocked with various cell tissues (pit aspirations) and there were micro-cracks on the pit edges. Previous studies showed that heat treatment caused some cracks and pit aspirations due to deterioration between wood cell layers (Boonstra *et al.* 2006; Gündüz and Aydemir 2009; Kaygın *et al.* 2009; Doğu *et al.* 2010; Awoyemi and Jones 2011; Salca and Hiziroglu 2014; Ling *et al.* 2016; Aytakin and Yazıcı 2021). As a result, the study showed that the heat treatment might have caused a major deterioration in the structural and morphological properties of the wood materials.

CONCLUSIONS

Beech and Uludag fir wood materials were thermally treated at 170, 190, and 210 °C for 4 h. The physical, mechanical, morphological, thermal, and structural properties of the heat-treated wood were determined, and the deformation analysis during the mechanical test and the strain distribution during the heat treatment process were investigated.

1. Digital image correlation (DIC) was effectively utilized in both mechanical testing and heat treatment, enabling strain mapping in three directions of heat-treated wood. The DIC results showed that the stress distribution intensified in the various areas for heat-treated woods.
2. The heat treatment increased the wood materials' thermal and physical properties, but it also reduced their mechanical properties due to the occurrence of micro-cracks and collapses in the wood cells.
3. The chemical structure did not change with the heat treatment, as indicated by the analysis conducted with Fourier transform infrared (FT-IR) spectroscopy and X-ray diffraction (XRD). The crystallinity of the samples generally increased as temperature increased. As a result, while the heat treatment improved the physical and thermal properties, mechanical properties decreased.

4. When accounting for the color changes and increased dimensional stability, it can be said that the heat-treated wood materials are an alternative product to indoor decoration products and decorative structural panels.

ACKNOWLEDGMENTS

This study was supported by the Scientific and Technological Research Council (TUBITAK) of Turkey (2209-A BİDEB, Funding Number: 1919B011904353).

REFERENCES CITED

- Altgen, M., Uimonen, T., and Rautkari, L. (2018). "The effect of de- and re-polymerization during heat-treatment on the mechanical behavior of Scots pine sapwood under quasi-static load," *Polymer Degradation and Stability* 147, 197-205. DOI: 10.1016/j.polymdegradstab.2017.12.007
- Awoyemi, L., and Jones, I. P. (2011). "Anatomical explanations for the changes in properties of western red cedar (*Thuja plicata*) wood during heat treatment," *Wood Science and Technology* 45(2), 261-267. DOI: 10.1007/s00226-010-0315-9
- Aydemir, D., Gunduz, G., and Onat, S. M. (2010). "The impacts of heat treatment on lap joint shear strength of black pine wood," *Journal of Adhesion* 86(9), 906-914.
- Aydemir, D., Gunduz, G., Altuntaş, E., Ertas, M., Turgut Şahin, H., and Hakki Alma, M. (2011). "Investigating changes in the chemical constituents and dimensional stability of heat-treated hornbeam and uludag fir wood," *BioResources* 6(2), 1308-1321. DOI: 10.15376/biores.6.2.1308-1321
- Aydemir, D., Kiziltas, A., Erbas Kiziltas, E., Gardner, D. J., and Gunduz, G. (2015). "Heat treated wood–nylon 6 composites," *Composites Part B: Engineering* 68, 414-423. DOI: 10.1016/j.compositesb.2014.08.040
- Aytekin, A., and Yazıcı, H. (2021). "Physical, anatomical, and photochemical analyses of some exotic wood species submitted to heat treatment," *Journal of Renewable Materials* 9(8), 1485-1501. DOI: 10.32604/jrm.2021.015768
- Barile, C., Casavola, C., and Pappalettera, G. (2019). "Digital image correlation comparison of damaged and undamaged aeronautical CFRPS during compression tests," *Materials* 12(2), article 249. DOI: 10.3390/ma12020249
- Bekhta, P., and Niemz, P. (2003). "Effect of high temperature on the change in color, dimensional stability and mechanical properties of spruce wood," *Holzforschung* 57(5), 539-546. DOI: 10.1515/HF.2003.080
- Bhuiyan, M. T. R., Hirai, N., and Sobue, N. (2001). "Effect of intermittent heat treatment on crystallinity in wood cellulose," *Journal of Wood Science* 47(5), 336-341. DOI: 10.1007/BF00766782
- Boonstra, M. J., Rijdsdijk, J. F., Sander, C., Tjeerdsma, B., Militz, H., Van Acker, J., Stevens, M., and Kegel, E. (2006). "Microstructural and physical aspects of heat-treated wood, Part 1. Softwoods," *Maderas. Ciencia y Tecnologia* 8(3), 193-208.
- Boonstra, M. J., and Tjeerdsma, B. (2006). "Chemical analysis of heat treated softwoods," *Holz als Roh- und Werkstoff* 64(3), 204-211. DOI: 10.1007/s00107-005-0078-4
- Boonstra, M. J., Van Acker, J., Tjeerdsma, B. F., and Kegel, E. V. (2007). "Strength

- properties of thermally modified softwoods and its relation to polymeric structural wood constituents,” *Annals of Forest Science* 64(7), 679-690. DOI: 10.1051/forest:2007048
- Brebu, M., and Vasile, C. (2010). “Thermal degradation of lignin—A review,” *Cellulose Chemistry and Technology* 44(9), 353-363.
- Brosse, N., El Hage, R., Chaouch, M., Pétrissans, M., Dumarçay, S., and Gérardin, P. (2010). “Investigation of the chemical modifications of beech wood lignin during heat treatment,” *Polymer Degradation and Stability* 95(9), 1721-1726. DOI: 10.1016/j.polymdegradstab.2010.05.018
- Camirero, M. A., Lopez-Pedrosa, M., Pinna, C., and Soutis, C. (2013). “Damage monitoring and analysis of composite laminates with an open hole and adhesively bonded repairs using digital image correlation,” *Composites Part B: Engineering* 53, 76-91. DOI: 10.1016/j.compositesb.2013.04.050
- Canal, L. P., González, C., Molina-Aldareguía, J. M., Segurado, J., and Lorca, J. (2012). “Application of digital image correlation at the microscale in fiber-reinforced composites,” *Composites Part A: Applied Science and Manufacturing* 43(10), 1630-1638. DOI: 10.1016/j.compositesa.2011.07.014
- Chen, C., Tu, D., Zhao, X., Zhou, Q., Cherdchim, B., and Hu, C. (2020). “Influence of cooling rate on the physical properties, chemical composition, and mechanical properties of heat-treated rubberwood,” *Holzforschung* 74(11), 1033-1042. DOI: 10.1515/hf-2019-0232
- Cheng, S., Huang, A., Wang, S., and Zhang, Q. (2016). “Effect of different heat treatment temperatures on the chemical composition and structure of Chinese fir wood,” *BioResources* 11(2), 4006-4016. DOI: 10.15376/biores.11.2.4006.4016
- Chien, Y.-C., Yang, T.-C., Hung, K.-C., Li, C.-C., Xu, J.-W., and Wu, J.-H. (2018). “Effects of heat treatment on the chemical compositions and thermal decomposition kinetics of Japanese cedar and beech wood,” *Polymer Degradation and Stability* 158, 220-227. DOI: 10.1016/j.polymdegradstab.2018.11.003
- Czajkowski, Ł., Olek, W., and Weres, J. (2020). “Effects of heat treatment on thermal properties of European beech wood,” *European Journal of Wood and Wood Products* 78(3), 425-431. DOI: 10.1007/s00107-020-01525-w
- Doğu, D., Tirak, K., Candan, Z., and Unsal, O. (2010). “Anatomical investigation of thermally compressed wood panels,” *BioResources* 5(4), 2640-2663. DOI: 10.15376/biores.5.4.2640-2663
- DIN 5033-1 (2017). “Colorimetry - Part 1: Basic terms of colorimetry,” German National Standard, Berlin, Germany.
- Esteves, B., and Pereira, H. (2009). “Wood modification by heat treatment: A review,” *BioResources* 4(1), 370-404. DOI: 10.15376/biores.4.1.370-404
- Esteves, B., Velez Marques, A., Domingos, I., and Pereira, H. (2013). “Chemical changes of heat treated pine and eucalypt wood monitored by FTIR,” *Maderas. Ciencia y Tecnología* 15(2), 245-258. DOI: 10.4067/S0718-221X2013005000020
- Faix, O., Meier, D., and Fortmann, I. (1990). “Thermal degradation products of wood,” *Holz als Roh- und Werkstoff* 48(7-8), 281-285. DOI: 10.1007/BF02626519
- Gennari, E., Picchio, R., and Lo Monaco, A. (2021). “Industrial heat treatment of wood: Study of induced effects on Ayous wood (*Triplochiton scleroxylon* K. Schum),” *Forests* 12(6), article 730. DOI: 10.3390/f12060730
- Gonultas, O., and Candan, Z. (2018). “Chemical characterization and ftir spectroscopy of thermally compressed eucalyptus wood panels,” *Maderas. Ciencia y Tecnología*

- 20(3), 431-442. DOI: 10.4067/S0718-221X2018005031301
- Gündüz, G., and Aydemir, D. (2009). "Some physical properties of heat-treated hornbeam (*Carpinus betulus* L.) wood," *Drying Technology* 27(5), 714-720. DOI: 10.1080/07373930902827700
- Gündüz, G., and Aydemir, D. (2009a). "The influence of mass loss on the mechanical properties of heat-treated black pine wood," *Wood Research* 54(4), 33-42.
- Gündüz, G., Aydemir, D., Kaygın, B., and Aytekin, A. (2009). "The effect of treatment time on dimensionally stability, moisture content and mechanical properties of heat treated Anatolian chestnut (*Castanea Sativa* Mill.) wood," *Wood Research* 54(2), 117-126.
- Gündüz, G., Aydemir, D., and Akgün, K. (2011). "The effects of tannin and thermal treatment on physical and mechanical properties of laminated chestnut wood composites," *BioResources* 6(2), 1543-1555.
- Gu, G., She, B., Xu, G., and Xu, X. (2017). "Non-uniform illumination correction based on the retinex theory in digital image correlation measurement method," *Optica Applicata* 47(2), 199-208.
- Hakkou, M., Pétrissans, M., Zoulalian, A., and Gérardin, P. (2005). "Investigation of wood wettability changes during heat treatment on the basis of chemical analysis," *Polymer Degradation and Stability* 89(1), 1-5. DOI: 10.1016/j.polymdegradstab.2004.10.017
- Harilal, R., Vyasrayani, C. P., and Ramji, M. (2015). "A linear least squares approach for evaluation of crack tip stress field parameters using DIC," *Optics and Lasers in Engineering* 75, 95-102. DOI: 10.1016/j.optlaseng.2015.07.004
- Hill, C. A. S. (2007). *Wood Modification: Chemical, Thermal and Other Processes*, John Wiley & Sons, Hoboken, NJ, USA.
- Inari, G. N., Pétrissans, M., Pétrissans, A., and Gérardin, P. (2009). "Elemental composition of wood as a potential marker to evaluate heat treatment intensity," *Polymer Degradation and Stability* 94(3), 365-368. DOI: 10.1016/j.polymdegradstab.2008.12.003
- ISO 13061-2 (2014). "Physical and mechanical properties of wood—test methods for small clear wood specimens—Part 2: Determination of density for physical and mechanical tests," International Organization for Standardization, Geneva, Switzerland.
- ISO 3133 (1975). "Wood – determination of ultimate strength in static bending," International Organization for Standardization, Geneva, Switzerland.
- ISO 3345 (1975). "Wood – determination of ultimate compression stress parallel to the grain," International Organization for Standardization, Geneva, Switzerland.
- ISO 3349 (1975). "Wood – determination of modulus of elasticity in static bending," International Organization for Standardization, Geneva, Switzerland.
- ISO 4287 (1997). "Geometrical product specifications (GPS)—surface texture: Profile method—terms, definitions and surface texture parameters," International Organization for Standardization, Geneva, Switzerland.
- ISO 4859 (1982). "Wood – determination of radial and tangential swelling," International Organization for Standardization, Geneva, Switzerland.
- Jeong, G. Y., and Park, M. J. (2016). "Evaluate orthotropic properties of wood using digital image correlation," *Construction and Building Materials* 113, 864-869. DOI: 10.1016/j.conbuildmat.2016.03.129
- Kaboorani, A., and Faezipour, M. (2009). "Effects of wood preheat treatment on thermal

- stability of HDPE composites,” *Journal of Reinforced Plastics and Composites* 28(24), 2945-2955. DOI: 10.1177/0731684408094064
- Kačíková, D., Kačík, F., Čabalová, I., and Ďurkovič, J. (2013). “Effects of thermal treatment on chemical, mechanical and colour traits in Norway spruce wood,” *Bioresource Technology* 144, 669-674. DOI: 10.1016/j.biortech.2013.06.110
- Karakus, K., Birbilen, Y., and Mengeloğlu, F. (2016). “Assessment of selected properties of LDPE composites reinforced with sugar beet pulp,” *Measurement* 88, 137-146. DOI: 10.1016/j.measurement.2016.03.039
- Karakuş, K., Aydemir, D., Gunduz, G., and Mengeloğlu, F. (2021). “Heat-treated wood reinforced high density polyethylene composites,” *Drvna industrija*, 72(3), 219-229.
- Kaygın, B., Gunduz, G., and Aydemir, D. (2009). “The effect of mass loss on mechanic properties of heat - Treated paulownia wood,” *Wood Research* 54(2), 101-108.
- Kaygın, B., Gündüz, G., and Aydemir, D. (2009). “Some physical properties of heat-treated paulownia (*Paulownia elongata*) wood,” *Drying Technology* 27(1), 89-93.
- Korkut, D., Korkut, S., Bekar, I., Budakçı, M., Dilik, T., and Çakıcıer, N. (2008). “The effects of heat treatment on the physical properties and surface roughness of Turkish Hazel (*Corylus colurna* L.) wood,” *International Journal of Molecular Sciences* 9(9), 1772-1783. DOI: 10.3390/ijms9091772
- Kubojima, Y., Okano, T., and Ohta, M. (2000). “Bending strength and toughness of heat-treated wood,” *Journal of Wood Science* 46(1), 8-15. DOI: 10.1007/BF00779547
- Kučerová, V., Lagaña, R., Výbohová, E., and Hýrošová, T. (2016). “The effect of chemical changes during heat treatment on the color and mechanical properties of fir wood,” *BioResources* 11(4), 9079-9094. DOI: 10.15376/biores.11.4.9079-9094
- Kučerová, V., and Výbohová, E. (2014). “Changes of cellulose in hydrolysis of willow (*Salix alba* L.) wood,” *Chemické Listy* 108(11), 1084-1089.
- Li, T., Cheng, D., Avramidis, S., Wålinder, M. E. P., and Zhou, D. (2017). “Response of hygroscopicity to heat treatment and its relation to durability of thermally modified wood,” *Construction and Building Materials* 144, 671-676. DOI: 10.1016/j.conbuildmat.2017.03.218
- Ling, Z., Ji, Z., Ding, D., Cao, J., and Xu, F. (2016). “Microstructural and topo chemical characterization of thermally modified poplar (*Populus cathayana*) cell wall,” *BioResources* 11(1), 786-799. DOI: 10.15376/biores.11.1.786-799
- Luis Gómez-Royuela, J., Majano-Majano, A., José Lara-Bocanegra, A., and Reynolds, T. P. S. (2021). “Determination of the elastic constants of thermally modified beech by ultrasound and static tests coupled with 3D digital image correlation,” *Construction and Building Materials* 302, article ID 124270. DOI: 10.1016/j.conbuildmat.2021.124270
- Marková, I., Hroncova, E., Tomaskin, J., and Turekova, I. (2018). “Thermal analysis of granulometry selected wood dust particles,” *BioResources* 13(4), 8041-8060. DOI: 10.15376/biores.13.4.8041-8060
- Martinka, J., Hroncová, E., Chrebet, T., and Balog, K. (2014). “The influence of spruce wood heat treatment on its thermal stability and burning process,” *European Journal of Wood and Wood Products* 72(4), 477-486. DOI: 10.1007/s00107-014-0805-9
- Mburu, F., Dumarçay, S., Bocquet, J. F., Petrissans, M., and Gérardin, P. (2008). “Effect of chemical modifications caused by heat treatment on mechanical properties of *Grevillea robusta* wood,” *Polymer Degradation and Stability* 93(2), 401-405. DOI: 10.1016/j.polymdegradstab.2007.11.017
- Mitsui, K., Inagaki, T., and Tsuchikawa, S. (2008). “Monitoring of hydroxyl groups in

- wood during heat treatment using NIR spectroscopy,” *Biomacromolecules* 9(1), 286–288. DOI: 10.1021/bm7008069
- Nhacila, F., Siteo, E., Uetimane, E., Manhica, A., Egas, A., and Möttönen, V. (2020). “Effects of thermal modification on physical and mechanical properties of Mozambican *Brachystegia spiciformis* and *Julbernardia globiflora* wood,” *European Journal of Wood and Wood Products* 78(5), 871-878. DOI: 10.1007/s00107-020-01576-z
- Nuopponen, M., Vuorinen, T., Jämsä, S., and Viitaniemi, P. (2005). “Thermal modifications in softwood studied by FT-IR and UV resonance Raman spectroscopies,” *Journal of Wood Chemistry and Technology* 24(1), 13-26. DOI: 10.1081/WCT-120035941
- De Oliveira Araújo, S., Rocha Vital, B., Oliveira, B., Oliveira Carneiro, A. de C., Lourenço, A., and Pereira, H. (2016). “Physical and mechanical properties of heat treated wood from *Aspidosperma populifolium*, *Dipteryx odorata* and *Mimosa scabrella*,” *Maderas. Ciencia y Tecnología* 18(1), 143-156. DOI: 10.4067/S0718-221X2016005000015
- Pan, B., Qian, K., Xie, H., and Asundi, A. (2009). “Two-dimensional digital image correlation for in-plane displacement and strain measurement: A review,” *Measurement Science and Technology* 20(6), article ID 062001. DOI: 10.1088/0957-0233/20/6/062001
- Pelaez-Samaniego, M. R., Yadama, V., Lowell, E., and Espinoza-Herrera, R. (2013). “A review of wood thermal pretreatments to improve wood composite properties,” *Wood Science and Technology* 47(6), 1285-1319. DOI: 10.1007/s00226-013-0574-3
- Percin, O., Peker, H., and Atilgan, A. (2016). “The effect of heat treatment on the some physical and mechanical properties of beech (*Fagus orientalis* lipsky) wood,” *Wood Research* 61(3), 443-456.
- Priadi, T., and Hiziroglu, S. (2013). “Characterization of heat treated wood species,” *Materials & Design* 49, 575-582. DOI: 10.1016/j.matdes.2012.12.067
- Salca, E.-A., and Hiziroglu, S. (2014). “Evaluation of hardness and surface quality of different wood species as function of heat treatment,” *Materials & Design* (1980-2015) 62, 416-423. DOI: 10.1016/j.matdes.2014.05.029
- Tjeerdsma, B. F., Boonstra, M., Pizzi, A., Tekely, P., and Militz, H. (1998). “Characterisation of thermally modified wood: Molecular reasons for wood performance improvement,” *Holz als Roh- und Werkstoff* 56(3), 149-153. DOI: 10.1007/s001070050287
- Tjeerdsma, B. F., and Militz, H. (2005). “Chemical changes in hydrothermal treated wood: FTIR analysis of combined hydrothermal and dry heat-treated wood,” *Holz als Roh- und Werkstoff* 63(2), 102-111. DOI: 10.1007/s00107-004-0532-8
- Tumen, I., Aydemir, D., Gunduz, G., Uner, B., and Cetin, H. (2010). “Changes in the chemical structure of thermally treated wood,” *BioResources* 5(3), 1936-1944. DOI: 10.15376/biores.5.3.1936-1944
- Windeisen, E., Strobel, C., and Wegener, G. (2007). “Chemical changes during the production of thermo-treated beech wood,” *Wood Science and Technology* 41(6), 523-536. DOI: 10.1007/s00226-007-0146-5
- Xing, D., Li, J., Wang, X., and Wang, S. (2016). “*In situ* measurement of heat-treated wood cell wall at elevated temperature by nanoindentation,” *Industrial Crops and Products* 87, 142-149. DOI: 10.1016/j.indcrop.2016.04.017

- Yang, H.-S., Wolcott, M. P., Kim, H.-S., and Kim, H.-J. (2005). "Thermal properties of lignocellulosic filler-thermoplastic polymer bio-composites," *Journal of Thermal Analysis and Calorimetry* 82(1), 157-160. DOI: 10.1007/s10973-005-0857-5
- Yoneyama, S., Koyanagi, J., and Arikawa, S. (2016). "Measurement of discontinuous displacement/strain using mesh-based digital image correlation," *Advanced Composite Materials* 25(4), 329-343. DOI: 10.1080/09243046.2015.1052131

Article submitted: December 29, 2023; Peer review completed: February 3, 2024;
Revised version received and accepted: March 14, 2024; Published: March 25, 2024.
DOI: 10.15376/biores.19.2.3010-3030